Molecular basis of positive allosteric modulation of GluN2B NMDA receptors by polyamines

Laetitia Mony[1], Shujia Zhu[1,2], Stéphanie Carvalho[1] and Pierre Paoletti[1,*]

[1]Institut de Biologie de l'Ecole Normale Supérieure (IBENS), Ecole Normale Supérieure, CNRS UMR 8197, INSERM U1024, Paris, France and [2]Shanghai Key Laboratory of Brain Functional Genomics, East China Normal University (ECNU), Shanghai, China

NMDA receptors (NMDARs) form glutamate-gated ion channels that have central roles in neuronal communication and plasticity throughout the brain. Dysfunctions of NMDARs are involved in several central nervous system disorders, including stroke, chronic pain and schizophrenia. One hallmark of NMDARs is that their activity can be allosterically regulated by a variety of extracellular small ligands. While much has been learned recently regarding allosteric inhibition of NMDARs, the structural determinants underlying positive allosteric modulation of these receptors remain poorly defined. Here, we show that polyamines, naturally occurring polycations that selectively enhance NMDARs containing the GluN2B subunit, bind at a dimer interface between GluN1 and GluN2B subunit N-terminal domains (NTDs). Polyamines act by shielding negative charges present on GluN1 and GluN2B NTD lower lobes, allowing their close apposition, an effect that in turn prevents NTD clamshell closure. Our work reveals the mechanistic basis for positive allosteric modulation of NMDARs. It provides the first example of an intersubunit binding site in this class of receptors, a discovery that holds promise for future drug interventions.

Introduction

Allosteric modulation of membrane receptors is widely viewed as a particularly promising strategy in the quest for novel treatments against disorders of the central nervous system (CNS). It relies on the observation that most receptors involved in neurotransmission, be it ionotropic or metabotropic, harbour binding sites for small ligands or ions distinct from the agonist binding sites and the occupancy of which alters receptor activity (orthosteric versus allosteric sites; see Bertrand and Gopalakrishnan, 2007; Niswender and

*Corresponding author. Institut de Biologie de l'Ecole Normale Supérieure (IBENS), Ecole Normale Supérieure, CNRS UMR 8197, INSERM U1024, 46 rue d'Ulm, Paris 75005, France.
Tel.: +33 14 432 3894; Fax: +33 14 432 3887;
E-mail: pierre.paoletti@ens.fr

Conn, 2010). The functional outcome of the binding of an allosteric ligand can be either a decrease or increase of the agonist-evoked response (negative versus positive allosteric modulation) depending on whether the receptors are stabilized in one of the inactive or active states. There are several advantages of targeting allosteric, rather than orthosteric, sites (Bertrand and Gopalakrishnan, 2007; Pin and Prezeau, 2007): first, they do not interfere with the biological patterns of receptor activity; second, allosteric modulators may not compete with a natural ligand as orthosteric ligands with the physiological agonist; third, they allow for subunit-specific modulation, something which is usually difficult to achieve at orthosteric sites given their high degree of conservation between receptor subtypes. For all these reasons, allosteric modulators represent pharmacological and therapeutic tools of great interest. This is the case in particular for compounds that interact with ionotropic glutamate receptors, a family of glutamate-gated ion channels that mediate excitatory synaptic transmission in the vertebrate CNS. Molecules capable of enhancing the activity of AMPA or NMDA receptors (NMDARs), the two principal classes of ionotropic glutamate receptors, have potential benefits for the treatment of cognitive deficits caused by neurodegenerative diseases, depression or schizophrenia (Lynch, 2004; Traynelis et al, 2010). However, while the molecular mechanisms of positive allosteric modulation of AMPA receptors have been dissected in much detail (Sun et al, 2002; Lynch, 2004; Jin et al, 2005), at NMDARs these mechanisms have yet to be elucidated.

The first discovered and best-characterized positive allosteric modulators of NMDARs are polyamines (Rock and Macdonald, 1995; Williams, 1997). Polyamines, such as spermine and spermidine, are polybasic aliphatic amines that are widely distributed throughout the body (Igarashi and Kashiwagi, 2010). They are found at high levels in the intracellular compartment where they regulate several cellular functions. In the CNS, there is also evidence that polyamines can be released into the extracellular medium in an activity-dependent manner. Once in the extracellular space, polyamines have the potential to modulate neuronal excitability by acting on various ion channels and receptors, including calcium channels and NMDARs (Rock and Macdonald, 1995; Williams, 1997; Mott et al, 2003). Extracellular polyamines have multiple effects on NMDAR responses including a voltage-dependent pore blockade, an increase in the apparent affinity for the coagonist glycine and a voltage-independent and glycine-independent potentiation that proceeds through a reduction of tonic proton inhibition and results in an enhancement of NMDAR responses recorded in saturating concentrations of agonists (McGurk et al, 1990; Lerma, 1992; Rock and MacDonald, 1992; Benveniste and Mayer, 1993; Williams et al, 1994; Traynelis et al, 1995). This latter effect of polyamines (hereafter named 'polyamine potentiation' for simplicity) has been most studied because of its unique subunit selectivity. NMDARs form heterotetrameric complexes usually consisting of two

GluN1 and two GluN2 subunits, of which there are four subtypes (Paoletti and Neyton, 2007; Traynelis *et al*, 2010). Only NMDARs containing the GluN2B subunit display polyamine potentiation (Williams *et al*, 1994; Zhang *et al*, 1994; Traynelis *et al*, 1995). Moreover, when the GluN1 subunit contains the exon 5 insert (GluN1-1b subunit), spermine potentiation is strongly diminished (Zhang *et al*, 1994; Traynelis *et al*, 1995).

Several studies have sought to determine the binding site and mechanism of polyamine potentiation of NMDARs. Numerous mutations that affect spermine sensitivity have been described (Williams *et al*, 1995; Kashiwagi *et al*, 1996, 1997; Gallagher *et al*, 1997; Masuko *et al*, 1999). These mutations are scattered throughout the sequence of both GluN1 and GluN2B subunits, therefore it has not been possible to identify a specific binding pocket for polyamines. Moreover, since most, if not all, of these mutations also alter receptor proton sensitivity, it is difficult to discriminate between direct binding effects and indirect effects through perturbations of the proton sensor. Even studies on purified isolated receptor domains have yielded mixed results, with some suggesting binding in the N-terminal domain (NTD) region (Han *et al*, 2008; see also Huggins and Grant, 2005) while other implicate the agonist binding domain (ABD) region (Stoll *et al*, 2007). Here, we use a combination of biochemical and electrophysiological analyses to address the mechanism and site of action of positive allosteric modulation of NMDARs by polyamines. We show that polyamines bind at a subunit–subunit interface and serve to stabilize NTD dimer assembly thus increasing the energy barrier for entering the inactive state of the receptor. These results define a novel mode of positive allosteric modulation of ionotropic glutamate receptors.

Results

Spermine potentiation shows strict subunit (GluN2B) selectivity even at acidic pH

Extracellular protons are potent allosteric inhibitors of NMDARs, and small changes of extracellular pH (pH_{ext}) can

significantly impact NMDAR current amplitudes (Traynelis *et al*, 1995). This is particularly true for receptors incorporating the GluN2B subunit and the GluN1 subunit lacking exon 5, which display a value of pH IC_{50} close to the physiological pH (7.3; Traynelis *et al*, 1995; Gielen *et al*, 2009). Spermine potentiation of GluN2B-containing receptors proceeds through the relief of tonic proton inhibition, shifting the pKa of the proton sensor towards more acidic values (Traynelis *et al*, 1995). Confirming the strong interrelation of the spermine and proton modulations, we observed that spermine potentiation massively increases when extracellular pH decreases (Figure 1A): thus, while at pH 7.3 200 μM spermine modestly potentiated GluN1/GluN2B responses (Williams *et al*, 1994) ($I_{spermine}/I_0 = 1.33 \pm 0.06$, $n = 5$; holding potential of −60 mV), at pH 6.3, the current increase was greater than nine-fold ($I_{spermine}/I_0 = 9.3 \pm 0.7$, $n = 4$). At alkaline pH (8.3), in contrast, spermine potentiation was absent; instead an inhibitory effect due to (voltage-dependent) spermine pore block was clearly evidenced ($I_{spermine}/I_0 = 0.6 \pm 0.1$, $n = 5$). Accordingly, in order to compare the spermine sensitivity of different NMDAR constructs, we decided to perform a spermine sensitivity assay in which 200 μM spermine was applied at pH 6.5 to maximize the spermine-induced potentiation.

Previous studies performed at physiological pH ($\sim$7.3) showed that spermine selectively potentiates NMDARs containing the GluN2B subunit (Williams *et al*, 1994; Zhang *et al*, 1994; Traynelis *et al*, 1995). We found that this subunit specificity was preserved in our assay at acidic pH. Indeed, while GluN2B-containing receptors where strongly potentiated (eight-fold), no potentiation was detected on GluN2A-, GluN2C- and GluN2D-containing receptors (Figure 1B). At pH 6.5, all NMDAR subtypes show marked tonic inhibition by protons (Traynelis *et al*, 1995; Gielen *et al*, 2009). Our results therefore suggest that spermine selectivity for GluN2B-containing receptors does not arise from a weak tonic proton inhibition of the other receptor subtypes, but rather from an absence of the potentiating spermine binding site in these subtypes.
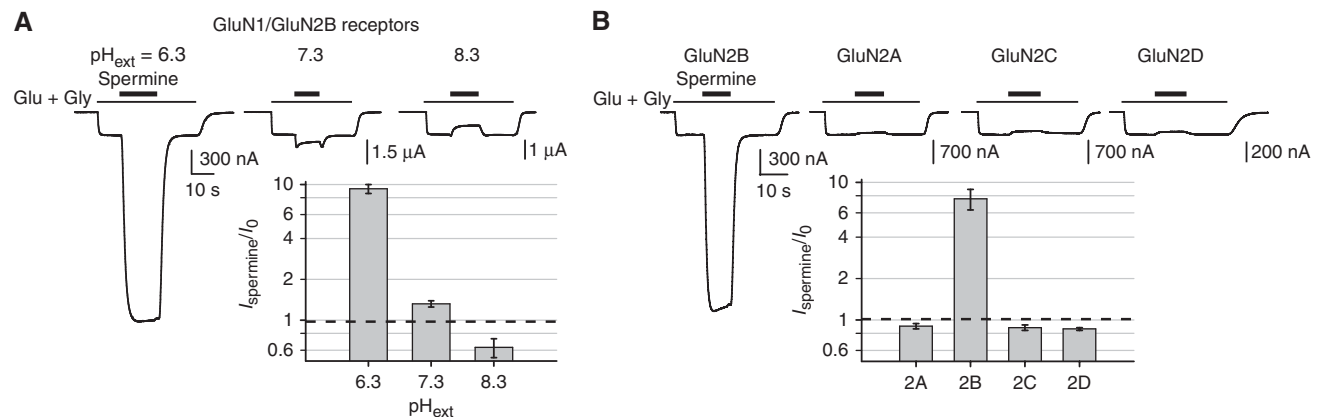

Figure 1 Properties of the glycine-independent and voltage-independent spermine potentiation. (**A**) The extent of spermine potentiation is greatly magnified by decreasing extracellular pH (pH_{ext}). Typical current traces obtained at three different pH_{ext} from oocytes expressing wild-type (wt) GluN1/GluN2B receptors. Spermine was applied at 200 μM. The bars above the current traces indicate the duration of agonists and spermine applications. Inset: Mean relative current amplitudes. Values are 9.3 ± 0.7 ($n = 4$), 1.33 ± 0.06 ($n = 5$) and 0.6 ± 0.1 ($n = 5$) at pH_{ext} of 6.3, 7.3 and 8.3, respectively. (**B**) Spermine potentiation is GluN2B specific. Typical current traces obtained at $pH_{ext} = 6.5$ from oocytes expressing NMDARs incorporating wt GluN1 and either one of the four wt GluN2 subunits. Spermine was applied at 200 μM. Inset: mean relative current amplitudes. Values are 0.90 ± 0.04 ($n = 17$), 8.0 ± 1.6 ($n = 50$), 0.88 ± 0.04 ($n = 7$) and 0.86 ± 0.02 ($n = 7$) for GluN2A-, GluN2B-, GluN2C- and GluN2D-containing receptors, respectively. The dashed line in the bar graphs indicates the lack of spermine effect ($I_{spermine}/I_0 = 1$).

Both GluN1 and GluN2B NTDs control spermine sensitivity

We next sought to identify the molecular determinants responsible for the spermine potentiation. We first recorded from receptors lacking the entire GluN1 or GluN2B NTD. Deletion of either NTD completely abolished potentiation by 200 μM spermine (Figure 2A and B), indicating that both GluN1 and GluN2B NTDs are required for spermine sensitivity. Spermine potentiation was also completely suppressed by replacing either the GluN2B NTD or the GluN2B NTD together with the short linker L connecting the NTD to the ABD, a region previously shown to be important in controlling receptor activity (Gielen *et al*, 2009; Yuan *et al*, 2009), by the corresponding residues of the spermine-insensitive GluN2A subunit (GluN2B-2A(NTD) and GluN2B-2A(NTD + L) subunits; Figure 2A and B). Conversely, swapping GluN2A and GluN2B NTDs (GluN2A-2B(NTD) subunit) conferred some spermine sensitivity onto GluN1/GluN2A receptors (Figure 2A and B). This gain-of-function phenotype could be further reinforced by increasing the chimera length to include the GluN2B linker segment (GluN2A-2B(NTD + L) subunit; Figure 2A and B). In contrast, transplanting the linker segment alone was insufficient to confer spermine sensitivity (Figure 2B). The systematic determination of proton sensitivity of the mutant receptors (Supplementary Figure S1A) also revealed that the observed changes in spermine sensitivity were uncorrelated to the changes in proton sensitivity. Together, these results provide strong support for the NTD region of GluN1/GluN2B receptors being the locus of spermine binding.

To further investigate the role of the GluN2B NTD and linker L on spermine sensitivity, we performed full spermine dose–response curves for the two chimeras containing the GluN2B NTD. To control for the differential proton sensitivities of the various constructs, spermine dose–response curves were performed at identical level of proton inhibition (96% proton inhibition, see Materials and methods). The spermine sensitivity of GluN1wt/GluN2A-2B(NTD + L) receptors was close to that of wild-type GluN1/GluN2B receptors, with EC_{50} values differing by only approximately two-fold (260 versus 127 μM) and levels of maximal potentiation almost identical ($\sim$11-fold; Figure 2C). Interestingly, the chimera in which only GluN2B NTD was transferred to the GluN2A subunit also showed a moderate ($\sim$3-fold) shift in EC_{50} compared with wt receptors, but the maximal potentiation was much decreased (4.9-fold; Figure 2C). These results demonstrate that the GluN2B NTD region contains key determinants for spermine potentiation. Moreover, they also indicate that the GluN2B linker, which is unable to induce spermine potentiation on its own (Figure 2B), has an
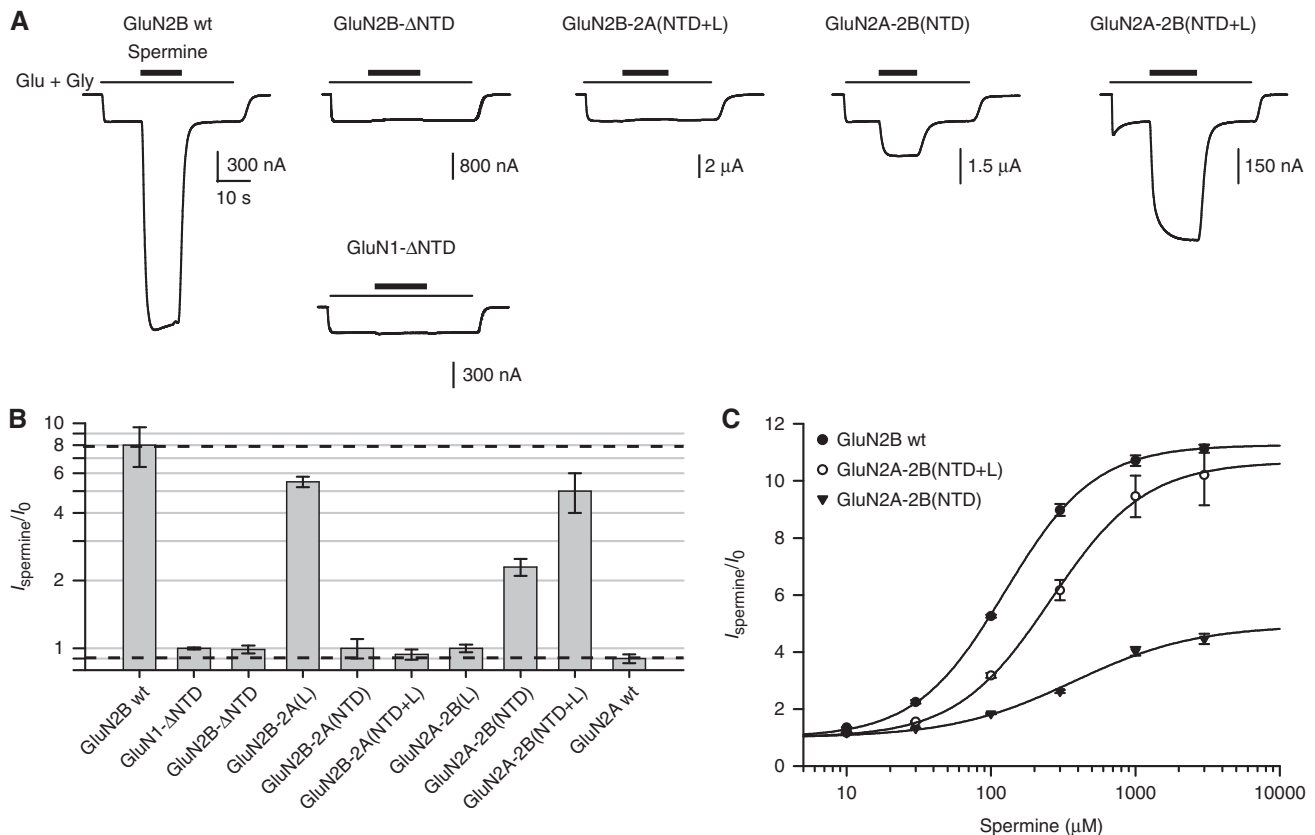

Figure 2 Both GluN1 and GluN2B NTDs are required for spermine potentiation. (**A**) Typical current traces from oocytes expressing receptors incorporating wild-type GluN1 and different chimeric GluN2 subunits, or YFP-GluN2B and a NTD-deleted GluN1 subunit (GluN1-ΔNTD) (lower trace; see Materials and methods). Spermine was applied at 200 μM; $pH_{ext} = 6.5$. (**B**) Summary of the spermine-induced effects. Values are (from left to right): 8.0 ± 1.6 ($n = 50$), 1.00 ± 0.01 ($n = 5$), 0.99 ± 0.04 ($n = 8$), 5.5 ± 0.3 ($n = 5$), 1.0 ± 0.1 ($n = 11$), 0.94 ± 0.05 ($n = 16$), 1.00 ± 0.04 ($n = 7$), 2.3 ± 0.2 ($n = 8$), 5.1 ± 1.1 ($n = 8$) and 0.90 ± 0.04 ($n = 17$). (**C**) Spermine dose–response curves of receptors containing GluN2B wt, GluN2A-2B(NTD) or GluN2A-2B(NTD + L) subunits. The spermine EC_{50}, maximal potentiation and Hill coefficient are, respectively: 127 ± 5 μM, 11.4 ± 0.3 and 1.40 ± 0.08 ($n = 6$) for wt GluN1/GluN2B receptors; 260 ± 30 μM, 11.0 ± 1.0 and 1.33 ± 0.07 ($n = 5$) for GluN1 wt/GluN2A-2B(NTD + L) receptors and 370 ± 30 μM, 4.9 ± 0.2 and 1.03 ± 0.05 ($n = 5$) for GluN1 wt/GluN2A-2B(NTD) receptors.

important role in transducing spermine binding into alterations of channel gating. The importance of the GluN2B linker in the coupling to the downstream gating machinery was further confirmed by assessing the spermine sensitivity of GluN1/GluN2B-2A(L) receptors, which revealed a decreased maximal potentiation but an apparent affinity for spermine only modestly affected (~1.5-fold; Figure 2B; Supplementary Figure S1B).

Spermine binds at a putative lower lobe NTD dimer interface between GluN1 and GluN2B subunits

Polyamines are polycationic molecules that usually interact with multiple acidic residues (aspartates, glutamates) on target proteins. This is the case, for instance, for PotD, the primary receptor of the polyamine transport system in bacteria and for which the structure has been solved in complex with spermidine (Sugiyama *et al*, 1996). We therefore looked for regions in GluN1 and GluN2B NTDs that contain clusters of negatively charged residues. A stretch of a few tens of amino acids highly enriched in acidic residues is found in both GluN1 and GluN2B NTDs in a region located between β-strands 6 and 8 and encompassing α-helices 5 and 6 and

β-strand 7 (according to the crystal structures of GluN1 and GluN2B NTDs; Karakas *et al*, 2009; Farina *et al*, 2011; Figure 3A and B). These regions, coined the β6–β8 regions, are interesting for several reasons: first, they contain multiple residues (mainly glutamates) that, when mutated, alter proton and spermine sensitivity (red residues in Figure 3A and circled residues in Figure 3C; Gallagher *et al*, 1997; Masuko *et al*, 1999; see Supplementary Figure S2); second, the corresponding region of the spermine-insensitive GluN2A subunit lacks several of the negatively charged residues found in GluN2B (Figure 3A and see electrostatic potential surface in Supplementary Figure S3); third, in domains with a related leucine/isoleucine/valine binding protein (LIVBP)-like fold, the β6–β8 region constitutes a large surface forming a lateral face of the domain lower lobe (Kunishima *et al*, 2000; He *et al*, 2001; Tsuchiya *et al*, 2002; Figure 3C). In AMPA and kainate receptors, this region is mostly hydrophobic and participates in a solvent-buried interface involved in NTD dimerization (Clayton *et al*, 2009; Jin *et al*, 2009; Kumar *et al*, 2009; Kumar and Mayer, 2010; but see Sukumaran *et al*, 2011). In NMDARs, however, many of these hydrophobic residues are replaced by hydrophilic or charged
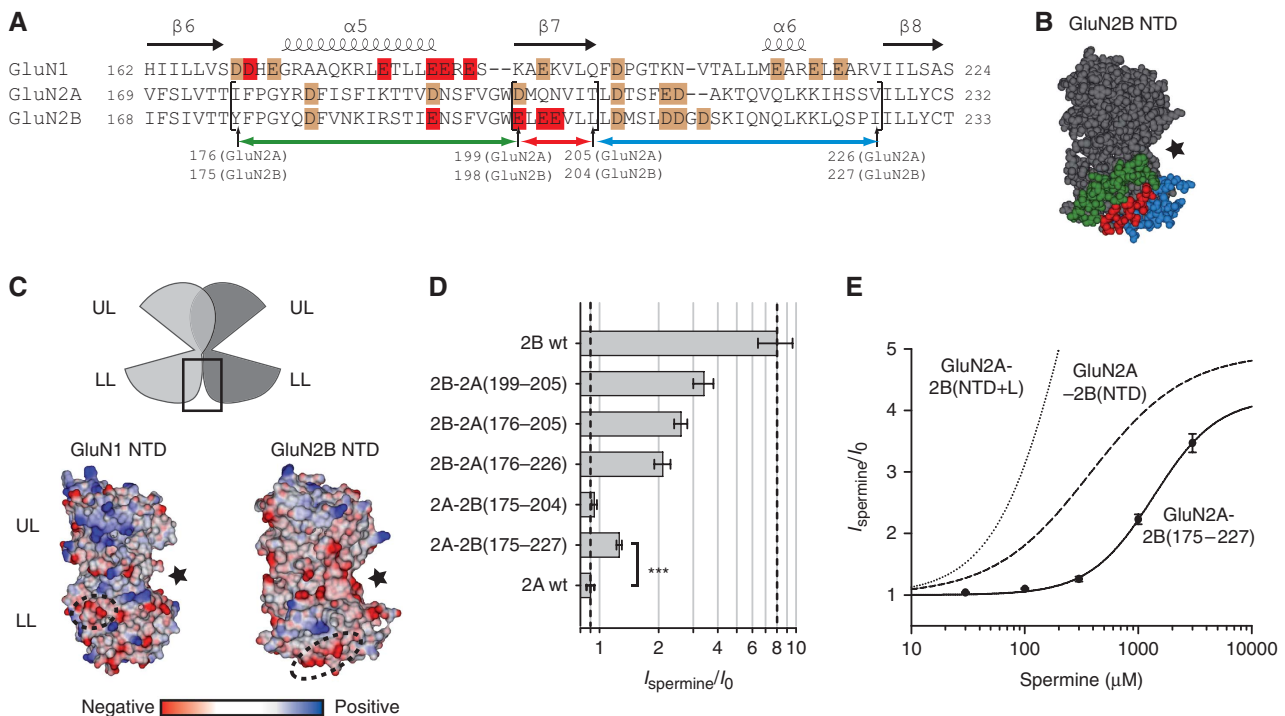

Figure 3 The β6–β8 region in the lower lobe of GluN2B NTD is critical for spermine potentiation. (**A**) Sequence alignment of the β6–β8 regions of GluN1, GluN2A and GluN2B subunits. Indicated α-helices (coils) and β-strands (arrows) are from GluN2B NTD crystal structure (pdb 3JPW; Karakas *et al*, 2009). Secondary structures are numbered according to the secondary structures of the AMPA GluA2 NTD (Jin *et al*, 2009). Red boxes correspond to acidic residues previously shown to influence spermine sensitivity (Masuko *et al*, 1999). Other acidic residues located in the β6–β8 region are highlighted by orange boxes. Limits of the different GluN2A/GluN2B NTD chimeras are represented by brackets and coloured arrows. (**B**) CPK (Corey–Pauling–Koltun) representation of GluN2B NTD (pdb 3JPW; Karakas *et al*, 2009) viewed from its putative dimerization face. The star indicates the position of the domain interlobe cleft. The green, red and blue represent the different regions exchanged between GluN2A and GluN2B in the chimeras (see corresponding coloured arrows in (**A**)). (**C**) (Top) Schematic representation of a dimer of LIVBP-like domains. The area corresponding to the β6–β8 regions of GluN1 and GluN2B NTDs is squared. (Bottom) Electrostatic potential surface of GluN1 (pdb: 3Q41; Farina *et al*, 2011) and GluN2B NTDs (pdb 3JPW; Karakas *et al*, 2009) viewed from their putative dimerization face. Stars indicate the position of the domain interlobe cleft. Note the high density of negative charges in the lobe 2 dimerization face of both GluN1 and GluN2B NTDs. Dashed circles represent the clusters of residues highlighted in red in (**A**). UL, upper lobe; LL, lower lobe. (**D**) Spermine sensitivities of the different β6–β8 chimeras. Values are, from top to bottom: 3.4 ± 0.4 ($n=8$), 2.6 ± 0.2 ($n=7$), 2.1 ± 0.2 ($n=8$), 0.94 ± 0.03 ($n=10$) and 1.28 ± 0.05 ($n=11$). ***$P < 0.001$ (Student's *t*-test). (**E**) Spermine dose–response curve of GluN1 wt/GluN2A-2B(175–227) receptors. The spermine EC_{50}, maximal potentiation and Hill coefficient are, respectively: 1.36 ± 0.08 mM, 4.2 ± 0.2 and 1.54 ± 0.05 ($n=5$). The dashed and dotted curves represent spermine dose–response curves for GluN1 wt/GluN2A-2B(NTD) and GluN1 wt/GluN2A-2B(NTD+L) receptors, respectively (replotted from Figure 2C).

residues, strongly suggesting an increased solvent accessibility (Figure 3C). With all these considerations in mind, we hypothesized that polyamines may bind at an NTD interface between GluN1 and GluN2B subunits through interactions with β6–β8 residues from both subunits.

We obtained evidence for a critical contribution of the β6–β8 region of GluN2B NTD in the control of spermine sensitivity by constructing chimeras in which parts of the β6–β8 region were swapped between GluN2B and GluN2A subunits. Introducing seven GluN2A residues that form the putative β7-strand into GluN2B (GluN1wt/GluN2B-2A (199–205) receptors; Figure 3A and red region in Figure 3B) resulted in a marked (two-fold) decrease of the potentiation induced by 200 μM spermine (Figure 3D). Interestingly, this small region contains two glutamates, GluN2B E200 and E201 that, in GluN2A, are replaced by neutral residues (Q201 and N202). Introduction of longer parts of the β6–β8 region of GluN2A NTD into GluN2B NTD further decreased spermine sensitivity, although without completely abolishing it (Figure 3D; green and blue regions). Noteworthily, receptors containing the chimeric subunits GluN2B-2A(199–205) and GluN2B-2A(176–205) showed a pH sensitivity close to wild-type GluN2B receptors (Supplementary Figure S4), indicating that the decrease in the spermine sensitivity of these mutant receptors likely reflects a modification of the spermine binding site rather than of the proton sensor. Exchanging the β6–β8 region between GluN2A and GluN2B was sufficient to confer spermine sensitivity to the chimeric GluN1/GluN2A-2B(175–227) receptors ($I_{spermine}/I_0 = 1.28 \pm 0.05$, $n = 11$; Figure 3D). Replacement of the full β6–β8 region was necessary, however, since no spermine potentiation was observed with a smaller chimera spanning α-helix 5 and β-strand 7 (GluN1/GluN2A-2B(175–204); Figure 3A, green and red regions in Figure 3B). The full spermine dose–response curve for GluN1/GluN2A-2B(175–227) receptors revealed that, compared with the full NTD chimera, spermine displayed decreased potency (∼4-fold increase in EC_{50}) but induced comparable maximal potentiation (4.2-fold; Figure 3E). Paralleling their acquired sensitivity to spermine, GluN1/GluN2A-2B(175–227) receptors displayed enhanced proton sensitivity compared with GluN1/GluN2A receptors (Supplementary Figure S4). Taken together, these results demonstrate that the β6–β8 region of GluN2B contains key determinants involved in the GluN2B-specific spermine potentiation even if full recapitulation of GluN2B wild-type spermine sensitivity obviously requires additional determinants. Moreover, the gain-of-function phenotype of the GluN2A-2B(175–227) chimera strongly supports a model in which the β6–β8 region of GluN2B directly participates to the formation of the spermine binding site.

GluN1 and GluN2B NTDs form heterodimers

The results obtained so far support our contention that spermine binds at an interface between GluN1 and GluN2B NTDs. But does GluN1 NTD partner with GluN2B NTD in an intact receptor? There is little doubt that NMDAR NTDs assemble as dimers, similarly to LIVBP-like domains found in other multimeric membrane proteins (including the NTDs of AMPA and kainate receptors; Kunishima *et al*, 2000; He *et al*, 2001; Clayton *et al*, 2009; Jin *et al*, 2009; Kumar *et al*, 2009; Kumar and Mayer, 2010; Sukumaran *et al*, 2011). However, whether NMDARs NTDs form homo- or heterodi-

mers is still unclear and indirect evidence exists for either arrangement (Schorge and Colquhoun, 2003; Sobolevsky *et al*, 2009). We decided to address this issue by performing cross-linking experiments between residues located in the NTD β6–β8 regions of the GluN1 and GluN2B subunits. We first introduced cysteines in both regions hoping to induce the formation of a disulphide bridge between the two neighbouring NTDs. However, as revealed by non-reducing western blotting analysis of functional full-length receptors expressed in Xenopus oocytes, no dimer was observed (Figure 4A and B). Because in NMDARs, the NTD lower lobes are unlikely to pack as tightly as in AMPA and kainate receptors (see Discussion), we next attempted to cross-link GluN1 and GluN2B NTDs using methanethiosulfonate MTS-2-MTS (M2M), a short bi-functional thiol-reactive cross-linker (Armstrong *et al*, 2006; Figure 4A). Treatment of GluN1/GluN2B receptors with 2 mM M2M induced the formation of a high molecular weight band when cysteines were introduced in both GluN1 and GluN2B NTDs (Figure 4B). No such band was observed in wild-type receptors or in single cysteine mutant receptors (Figure 4B), demonstrating that M2M-induced NTD tethering occurs only between neighbouring GluN1 and GluN2B β6–β8 regions. Thus, GluN1 and GluN2B NTDs pair as heterodimers, not homodimers, and their lower lobes can be trapped facing each other within short distance (<8 Å, based on the estimated length of M2M).

Forcing close apposition of GluN1 and GluN2B NTD lower lobes increases receptor activity

What is the molecular mechanism underlying spermine potentiation of GluN2B-containing NMDARs? We and others have recently shown that the N-terminal regions of GluN2 subunits have a major influence on receptor activity by setting the maximal level of channel activity in a subunit-specific manner (Gielen *et al*, 2009; Yuan *et al*, 2009). The NTDs exert their influence by undergoing spontaneous (ligand-independent) oscillations between an open-cleft conformation, that favours channel opening, and a closed-cleft conformation, that favours channel closure (Gielen *et al*, 2008, 2009). Accordingly, GluN2B-containing receptors have a much lower maximal open probability (Po) than GluN2A-containing receptors (0.1 versus 0.5) because GluN2B NTD spends most of its time in a closed-cleft conformation while GluN2A NTD is mostly open (Gielen *et al*, 2009). Grounded in this NTD-driven gating control mechanism, we envisioned a model for spermine potentiation centred on the idea that spermine binding stabilizes an open-cleft conformation of GluN2B NTD, that is a 'high' Po state of the receptor. In this model, spermine binds at a dimer interface between GluN1 and GluN2B NTD lower lobes highly enriched in acidic residues (from facing GluN1 and GluN2B β6–β8 regions). By doing so, the polycationic spermine molecule alleviates the electrostatic repulsion between the NTD lower lobes thus preventing their separation and NTD cleft closure. To validate this model, we tested several predictions.

A first prediction is that maintaining GluN1 and GluN2B NTD lower lobes in close proximity should increase NMDAR activity. For that, we examined the functional effects of the short cross-linker M2M that induces covalent attachment of GluN1 and GluN2B NTD β6–β8 regions (see above and Figure 4B). Application of 0.2 mM M2M produced a strong
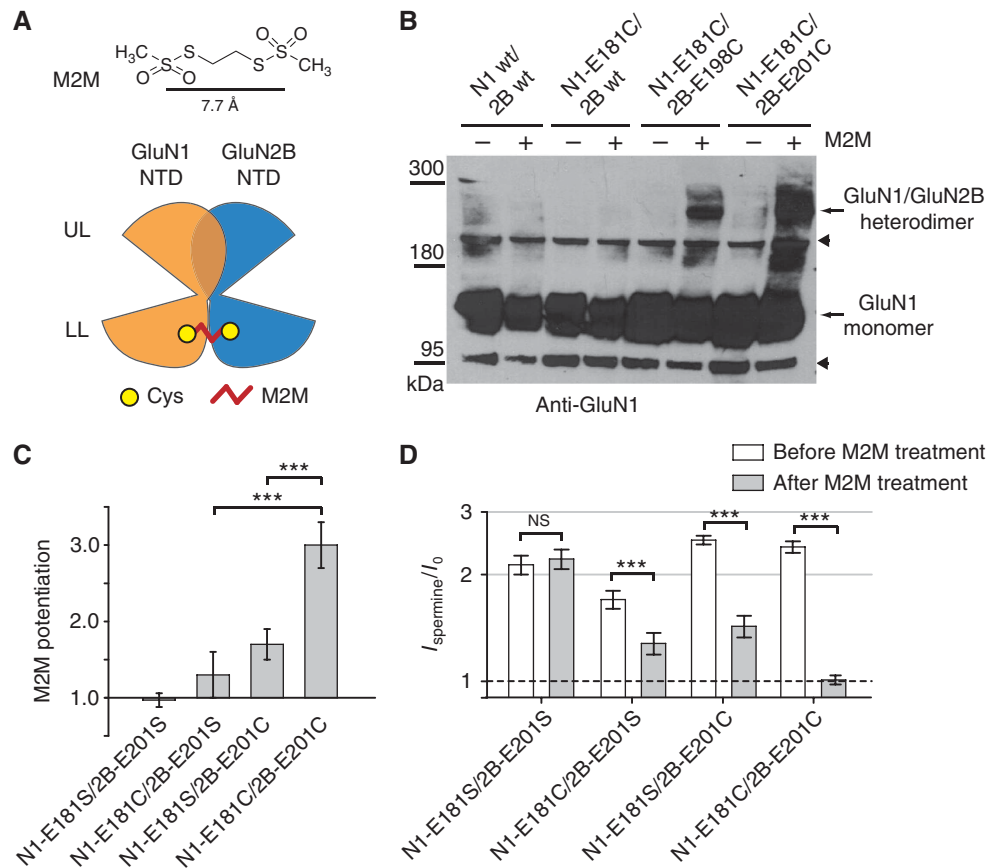
Figure 4 GluN1 and GluN2B NTDs assemble as heterodimers. (**A**) (Top) Chemical structure and length of M2M. (Bottom) Schematic depiction of the cross-linking experiment. (**B**) Western blots using an anti-GluN1 antibody on membrane fractions of Xenopus oocytes expressing four combinations of wt and mutated GluN1 and GluN2B subunits. Samples were run in non-reducing conditions after incubation of the intact oocytes in either 1% DMSO (−) or 2 mM M2M (+). The arrowheads indicate non-specific bands (also seen in non-injected oocytes). (**C**) Functional effects of M2M applications (0.2 mM, $pH_{ext} = 6.5$). Values are (from left to right): 0.97 ± 0.09 ($n = 4$), 1.3 ± 0.3 ($n = 6$), 1.7 ± 0.2 ($n = 8$) and 3.0 ± 0.3 ($n = 6$). ***$P < 0.001$ (Student's t-test). (**D**) Spermine sensitivities before and after treatment with 200 μM M2M. The dashed line represents the absence of spermine effect. Note the complete abolition of spermine potentiation after M2M treatment of GluN1-E181C/GluN2B-E201C receptors. Each bar corresponds to the mean value from 4 to 6 different cells. ***$P < 0.001$; NS, non-significant (Student's t-test).

and irreversible increase in currents carried by the double cysteine mutant GluN1-E181C/GluN2B-E201C receptors (3.0 ± 0.2-fold potentiation, $n = 6$). In contrast, no or little potentiation was observed with the control mutants, which contain either a single or no introduced cysteine (Figure 4C). The small potentiations observed with the single cysteine mutants likely result from the single-side attachment of M2M to the introduced cysteine as intersubunit cross-linking was not observed with these mutants in western blot analysis. Consistent with an occlusion of the spermine binding site, spermine potentiation of GluN1-E181C/GluN2B-E201C receptors was completely abolished after M2M treatment ($I_{spermine}/I_0 = 1.01 \pm 0.03$, $n = 6$, versus 2.39 ± 0.09, $n = 6$, before treatment), while the single cysteine mutants still retained some spermine sensitivity after M2M treatment ($I_{spermine}/I_0 = 1.28 \pm 0.09$, $n = 6$, for GluN1-E181C/GluN2B-201S receptors and 1.4 ± 0.1, $n = 4$, for GluN1-E181S/GluN2B-E201C receptors; Figure 4D). At the other extreme, spermine potentiation was left intact on non-reactive (serine mutant) receptors (Figure 4D). Taken together, these results fully support our hypothesis that separation of the GluN1 and GluN2B NTD lower lobes triggers entry of the receptors in a low Po state.

Introducing positive charges mimics spermine potentiation

A second prediction of our proposed mechanism for spermine potentiation is that reversing the polarity of some of the negative residues located at the lower lobe NTD dimer interface should increase receptor activity by decreasing the electrostatic repulsion between GluN1 and GluN2B NTDs. Acidic residues of the β6–β8 regions of GluN1 and GluN2B NTDs were mutated into positively charged residues (lysine or arginine). First, we verified that spermine sensitivity was affected by these mutations. Introduction of a single basic residue in either GluN1 or GluN2B β6–β8 region was sufficient to strongly reduce spermine sensitivity, as exemplified by GluN1-E181R/GluN2Bwt or GluN1wt/GluN2B-E201R receptors ($I_{spermine}/I_0 = 1.9 \pm 0.1$, $n = 4$, and 1.43 ± 0.08, $n = 11$, respectively, versus eight-fold for wild-type receptors; Figure 5A and B; Supplementary Figure S5). Even more dramatic was the effect when two or more positively charged residues, distributed on both subunits, were introduced. In such mutant receptors, spermine potentiation was in fact completely suppressed as exemplified by the double arginine mutant receptor GluN1-E181R/GluN2B-E201R ($I_{spermine}/I_0 = 0.83 \pm 0.07$, $n = 9$; Figure 5A and B; Supplementary
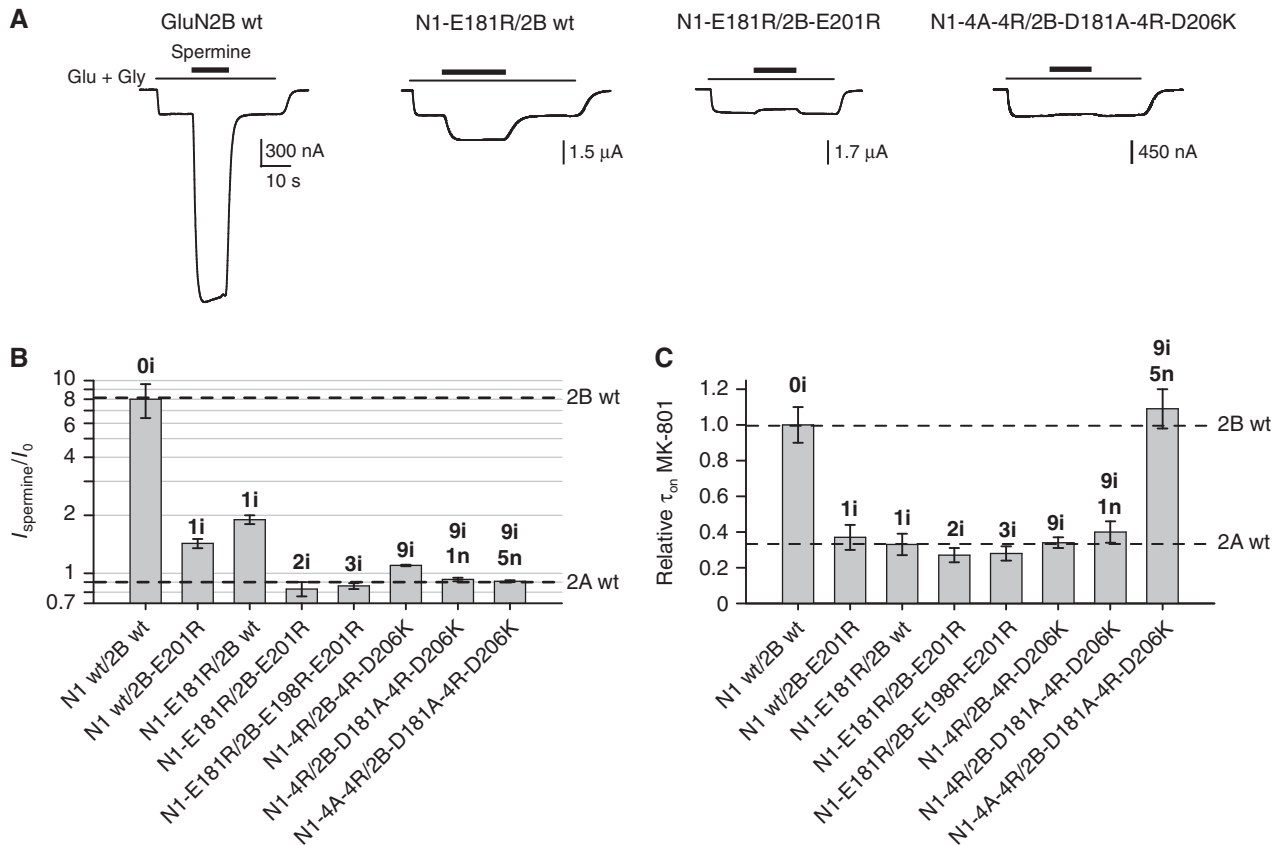
Figure 5 Mimicking spermine potentiation by introducing basic residues. (**A**) Typical current traces from oocytes expressing receptors in which acidic residues located in the putative lower lobe dimer interface between GluN1 and GluN2B NTDs were substituted by positively charged (arginine or lysine) or neutral (alanine) residues. Spermine was applied at 200 μM; $pH_{ext} = 6.5$. (**B**) Examples of spermine sensitivities of a series of mutant receptors substituted with positively charged residues at different GluN1 and GluN2B positions. Values are, from left to right: 8.0 ± 1.6 ($n = 50$), 1.43 ± 0.08 ($n = 9$), 1.9 ± 0.1 ($n = 4$), 0.83 ± 0.07 ($n = 9$), 0.86 ± 0.03 ($n = 4$), 1.10 ± 0.01 ($n = 5$), 0.93 ± 0.02 ($n = 6$) and 0.91 ± 0.01 ($n = 3$). The numbers in bold indicate the number of charge inversions (i) or charge neutralizations (n). (**C**) MK-801 inhibition kinetics of the mutant receptors described in (**B**). Onset time constants (τ_{on}) were normalized to the value obtained for wild-type GluN1/ GluN2B receptors. Values are, from left to right: 1.0 ± 0.1 ($n = 86$), 0.38 ± 0.07 ($n = 8$), 0.33 ± 0.06 ($n = 4$), 0.27 ± 0.04 ($n = 15$), 0.28 ± 0.04 ($n = 4$), 0.34 ± 0.03 ($n = 6$), 0.40 ± 0.06 ($n = 6$) and 1.1 ± 0.1 ($n = 6$).

Figure S5). Moreover, the effects on spermine sensitivity were consistently larger when the charges were inversed rather than neutralized (cysteine mutations; see Supplementary Figure S2), in agreement with an electrostatic-dependent mechanism.

Modifications of receptor activity were evaluated using the MK-801 approach, a method that allows estimations of Po through measurements of MK-801 inhibition kinetics (Rosenmund *et al*, 1993; Gielen *et al*, 2009). Converting one, two, three or more (up to nine) residues located in the lower lobe dimer interface of GluN1 and GluN2B NTDs into positively charged residues markedly increased receptor activity (Figure 5C; Supplementary Figure S6), as revealed by the much decreased MK-801 inhibition time constants (three-to four-fold decrease in τ_{on} compared with the wild-type value; Figure 5C). In fact, most arginine-mutated receptors had an estimated Po similar to that of wild-type GluN1/ GluN2A receptors, the NMDAR subtype with the highest Po (relative MK-801 τ_{on} of 0.34 ± 0.08, $n = 26$). Thus, introducing positive charges in the lower lobe dimer interface between GluN1 and GluN2B NTDs mimics the spermine-mediated increase in receptor channel activity.

If electrostatic repulsion between the negative charges lining the β6–β8 regions of GluN1 and GluN2B NTDs is the driving force that triggers the entry of NMDARs into a low

Po state, we hypothesized that inverting these charges in sufficient number may eventually restore Po to a low, wild-type like, value. This was indeed the case with the mutant receptor GluN1-4A-4R/GluN2B-D181A-4R-D206K, in which nine acidic residues were mutated into positively charged residues, and five others were neutralized into alanines (see Materials and methods). This receptor had an estimated Po very close to that of wild-type GluN1/GluN2B receptors (relative MK-801 τ_{on} of 1.1 ± 0.1, $n = 6$; Figure 5C), despite the fact that, as expected, its spermine sensitivity was completely abolished (Figure 5A and B). To our knowledge, this is the first report that spermine sensitivity and receptor activity can be uncorrelated, thus providing strong support for our model whereby spermine increases receptor activity by binding and shielding negative charges lining GluN1 and GluN2B NTD lower lobes.

Spermine stabilizes GluN2B NTD in an open-cleft conformation

A third prediction of our proposed mechanism for spermine potentiation is that spermine binding should render the separation of the NTD dimer lower lobes energetically less favourable, an effect that should translate into a shift of the GluN2B NTD open–close equilibrium towards the open state.

To assess the conformational state of GluN2B NTD, we evaluated the accessibility of a cysteine introduced deep in the NTD interlobe cleft (Figure 6A). For that purpose, we applied the bulky thiol-reactive reagent MTSPtrEA (200 μM; Figure 6B) to receptors containing a tyrosine-to-cysteine mutation at position 282 in GluN2B, a position buried in the closed structure of GluN2B NTD (Karakas et al, 2009). By attaching to the introduced cysteine, MTSPtrEA locks open the NTD thus increasing receptor Po (Gielen et al, 2009). Comparison of the kinetics of the MTSPtrEA-induced potentiations revealed that MTSPtrEA reacted faster in the presence of spermine than in its absence (MTSPtrEA τ_{on} of 9 ± 3 s, $n = 17$, and 18 ± 2 s, $n = 16$, respectively; Figure 6B and C). These results indicate that GluN2B NTD spends more time in an open conformation in the presence of spermine than in its absence. As expected from an increase in receptor Po by spermine, the amplitude of MTSPtrEA-induced potentiation was lower in the presence of spermine than in the absence of the modulator (Figure 6B and D). Finally, no potentiation was seen on the non-reactive control mutant receptors GluN1wt/GluN2B-Y282S, confirming the specificity of the MTSPtrEA-induced reaction (Figure 6D).

Discussion

Our results provide a molecular and mechanistic basis for the positive allosteric modulation of NMDARs by polyamines. We identify the NTD lower lobe GluN1/GluN2B dimer interface as a region critical for binding polyamines and decrypt the mechanism by which polyamines enhance receptor activity through stabilization of the NTD dimer assembly. We also reveal that in fully assembled GluN1/GluN2 NMDAR complexes, the NTDs associate as heterodimers similarly to ABDs (Furukawa et al, 2005; Gielen et al, 2008; Sobolevsky et al, 2009) providing important novel information about NMDAR architecture. Together with previous work on NTDs and their role in allosteric inhibition (Paoletti and Neyton, 2007; Mony et al, 2009a; Hansen et al, 2010 and see below), our work provides compelling evidence that the N-terminal region of NMDARs serves as a convergent target for small ligands acting as subunit-specific negative or positive allosteric modulators. It thus appears that the NTDs have a central role in controlling NMDAR activity and determining the pharmacological attributes of the various NMDAR subtypes.
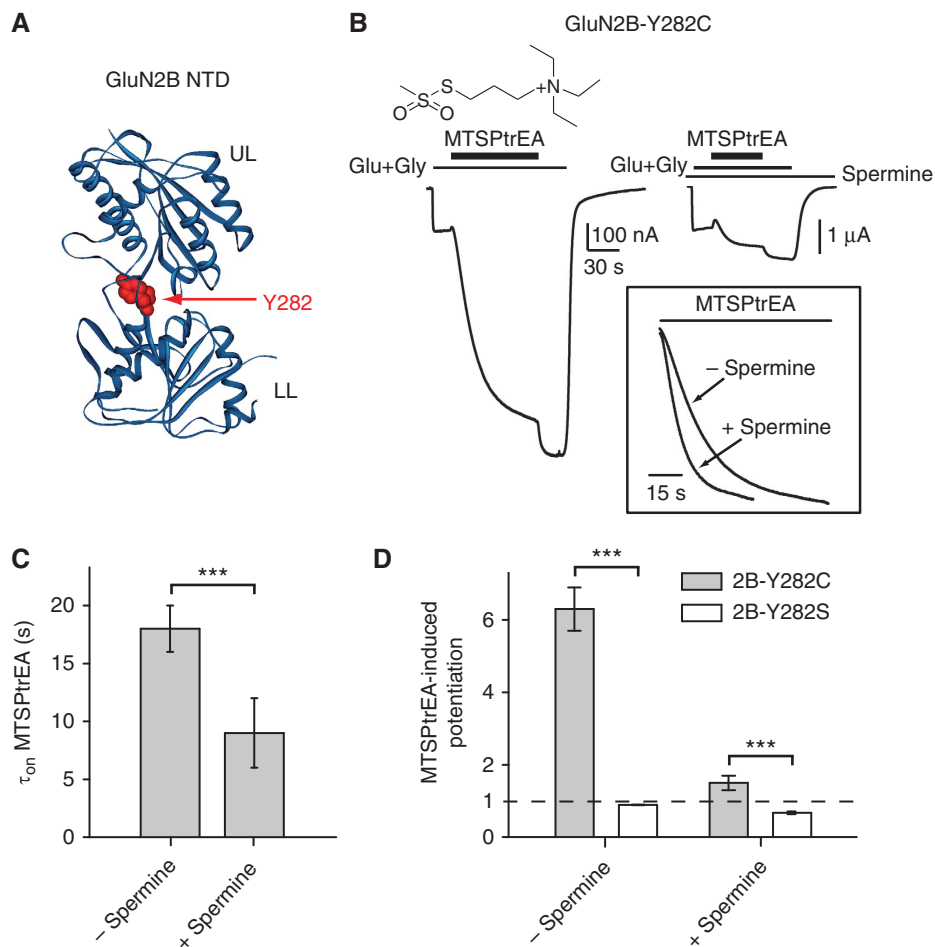

Figure 6 Spermine stabilizes an open-cleft conformation of GluN2B NTD. (**A**) Ribbon representation of GluN2B NTD (pdb: 3JPW; Karakas et al, 2009). The interlobe cleft residue Y282 is highlighted in red CPK. UL, upper lobe; LL, lower lobe. (**B**) Typical current traces from oocytes expressing GluN1wt/GluN2B-Y282C receptors during treatment with MTSPtrEA (200 μM) with or without spermine (200 μM). Inset: MTSPtrEA modification kinetics are faster in the presence of spermine (normalized currents). (**C**) Time constants of MTSPtrEA-induced potentiation (τ_{on} MTSPtrEA) of GluN1 wt/GluN2B-Y282C receptors. Mean values are 18 ± 2 s ($n = 16$) in the presence of spermine and 9 ± 3 s ($n = 17$) in its absence. ***$P < 0.001$ (Student's t-test). (**D**) Mean amplitudes of MTSPtrEA-induced potentiations on GluN1 wt/GluN2B-Y282C and GluN1 wt/GluN2B-Y282S receptors in the presence or absence of 200 μM spermine. Values are (from left to right): 6.3 ± 0.6 ($n = 16$), 0.89 ± 0.01 ($n = 3$), 1.6 ± 0.2 ($n = 16$) and 0.67 ± 0.04 ($n = 3$). ***$P < 0.001$ (Student's t-test).

Over 10 years of structure–function studies have established that NMDARs NTDs can sense their extracellular microenvironment by binding small ligands acting as subunit-specific allosteric inhibitors. Thus, GluN2A NTD forms a high-affinity (nM) binding site for the endogenous cation Zn^{2+} while GluN2B NTD also harbours a zinc-binding site (of µM affinity) and a binding site for the GluN2B-selective synthetic compounds ifenprodil and derivatives (Choi and Lipton, 1999; Low *et al*, 2000; Paoletti *et al*, 2000; Perin-Dureau *et al*, 2002; Rachline *et al*, 2005; Mony *et al*, 2009b). Zinc and ifenprodil have been proposed to bind the NTD interlobe cleft and promote domain closure by stabilizing a closed-cleft conformation. This conformational change then propagates to downstream elements of the receptor by pulling apart the ABD dimer interface, a motion that promotes receptor inhibition by uncoupling ABD closure to ion channel opening (Mayer, 2006; Gielen *et al*, 2008). The long-distance influence of the NTDs on channel gating can even occur independently of modulatory ligand binding through spontaneous close-to-open oscillations of GluN2 NTDs, an effect that accounts for the GluN2-specificity of receptor Po (Gielen *et al*, 2009; Yuan *et al*, 2009).

By integrating these data and the present results, we propose a unified model for negative and positive allosteric modulation of NMDARs via the NTDs (Figure 7). In this model, GluN1 and GluN2 NTDs primarily partner by upper lobe interactions. A GluN1/GluN2 NTD dimer can alternate between two conformational states, A (for 'active') and D (for 'desensitized-like') states. In the A state, GluN2B NTD is in an open-cleft conformation and GluN1 and GluN2B NTDs are closely associated, with their lower lobes close to each other. In the D state, because of NTD cleft closure, the lower lobes have swung apart rendering the NTD dimer more loosely packed. Both intra- and inter-protomer movements are thus operating in the transition from A to D states. Whether GluN1 NTD alternates between an open- and closed-cleft conformation is still unknown. Our data reveal that in GluN1/GluN2B receptors, electrostatics is a major
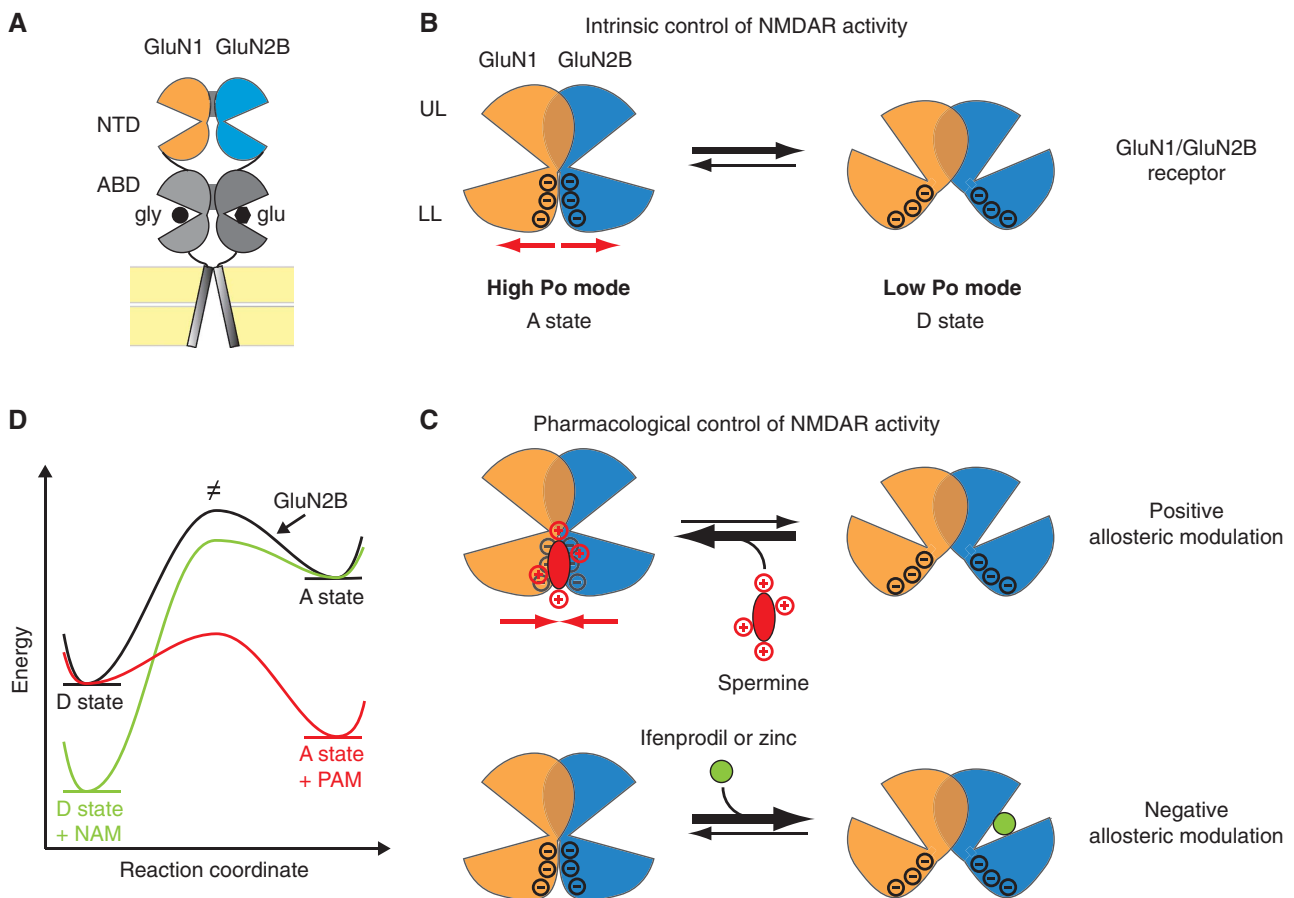

Figure 7 Proposed mechanism for allosteric control of GluN2B-containing NMDARs by the NTDs. (**A**) Schematic view of a heterodimer of GluN1 and GluN2B subunits. GluN1 NTD is represented in orange and GluN2B NTD in blue. GluN1 and GluN2B NTDs likely dimerize primarily through upper lobe interactions (see Text). (**B**) Intrinsic control of receptor activity. GluN1/GluN2B NTD dimer assembly undergoes spontaneous (ligand-independent) interconversions between conformation A, in which the NTDs are in an open state with their lower lobes closely apposed, and conformation D, in which the lower lobes have swung apart because of domain closure. The A conformation favours channel opening ('high Po' mode) while the D conformation promotes channel closure (i.e. receptor inhibition) by disrupting the ABD dimer interface ('low Po' mode; Gielen *et al*, 2008, 2009). In GluN1/GluN2B receptors, electrostatic repulsion (red arrows) between the lower lobes of GluN1 and GluN2B NTDs favours entry into the D state thus accounting for the low Po of this receptor subtype. UL, upper lobe; LL, lower lobe. (**C**) Pharmacological control of NMDAR activity. Polyamines such as spermine and spermidine shield the negative charges of the lower lobe NTD dimer interface and convert electrostatic repulsion into attraction (red arrows), thus stabilizing the dimer assembly in the high Po A state. In contrast, negative allosteric modulators like ifenprodil or zinc, which bind the GluN2B NTD cleft (Rachline *et al*, 2005; Karakas *et al*, 2009; Mony *et al*, 2009b), promote cleft closure and NTD lower lobes separation, thus favouring entry in the 'low Po' D state. (**D**) Energetic diagram summarizing the different conformational states of a GluN1/GluN2B NTD dimer in presence or in absence of negative allosteric modulators (NAM) and positive allosteric modulators (PAM). ≠, transition state.

driving force in controlling the A/D equilibrium. Indeed, we show that the numerous negative charges that are present in the β6–β8 regions of GluN1 and GluN2B NTD lower lobes repel each other, facilitating entry into the D state. Accordingly, in the absence of any allosteric modulator, GluN1/GluN2B receptors spend most of their time in the D state thus accounting for the low Po of GluN2B-containing receptors (Gielen *et al*, 2009; Yuan *et al*, 2009; Figure 7B and D). Conversely, GluN2A-containing receptors have a much higher Po in part because they lack several of the acidic residues present in GluN2B β6–β8 region. According to the model, any ligand that stabilizes the D state would act like a negative allosteric modulator. That is exactly what happens when zinc or ifenprodil binds GluN2A or GluN2B NTD and promotes NTD closure and lower lobe separation (Figure 7C and D). In contrast, polyamines such as spermine or spermidine act as positive allosteric modulators of GluN2B receptors by stabilizing the A state. These polyamines bind an acidic pocket at the NTD lower lobe GluN1/GluN2B dimer interface and alleviate the electrostatic repulsion between the two protomers (Figure 7C and D). Our data with GluN2A/ GluN2B chimeras show that, while the exchange of GluN2B β6–β8 region is sufficient to confer spermine potentiation, only the full exchange of the NTD plus NTD-ABD linker segment allows near complete transfer of spermine sensitivity (Figures 2 and 3). We interpret this result as evidence of the critical importance of a proper GluN1/Glu2B NTD dimer organization for maximal spermine sensitivity, something that may not be achieved by introducing the short GluN2B β6–β8 region in a GluN2A background (despite the acquired capability to bind spermine).

The proposed mechanism for bidirectional allosteric regulation of GluN2B NMDARs provides an explanation for the negative interaction that has been described between polyamines and zinc (Traynelis *et al*, 1998) or ifenprodil (with ifenprodil destabilizing the binding of spermine and vice versa; Kew and Kemp, 1998). Indeed, our model predicts that zinc- or ifenprodil-induced NTD cleft closure separates the lower lobes in a NTD dimer, an effect that spermine binding will oppose by 'gluing' together the two neighbouring NTDs. The observation that zinc or ifenprodil inhibition is relieved by spermine thus finds its mechanistic correlate. Both our results (Mony *et al*, 2009b and present work) and those of Kew and Kemp (1998) are consistent with a model of non-overlapping binding sites for spermine and ifenprodil on the GluN2B NTD (lower lobe versus interlobe cleft, respectively), though the precise identification of these two modulatory sites still awaits further structural studies. On native NMDARs, the counterbalancing effects of polyamines and zinc are likely to participate in the fine-tuning of NMDAR activity. Indeed, zinc ions are concentrated at many glutamatergic synapses in the CNS and, similarly to polyamines, can be released in the extracellular space following neuronal activity (Paoletti *et al*, 2009).

The mode of action of polyamines that we describe on NMDARs bears striking resemblance with the mode of action of Gd^{3+} ions at metabotropic glutamate receptors (mGluRs; Tsuchiya *et al*, 2002). The glutamate-binding domain of mGluRs is structurally related to NMDAR NTDs and also operates as dimers (Kunishima *et al*, 2000). A cluster of acidic residues makes the interactions between the two glutamate-binding domain lower lobes unfavourable; gadolinium binds this cluster and stabilizes the dimer in an active conformation, thus enhancing receptor activity (Tsuchiya *et al*, 2002). In natriuretic peptide receptors, also made of a pair of clamshell LIVBP-like domains, the activating natriuretic peptide binds a similar lower lobe dimer interface (He *et al*, 2001). Signalling through ligand binding to the lower lobe dimer interface appears therefore as a shared principle for many multimeric receptors containing LIVBP-like domains. For non-NMDA ionotropic glutamate receptors, the situation differs however. Indeed, crystal structures of AMPA and kainate NTDs show tightly associated dimers with extensive interactions involving both the upper and lower lobes (Clayton *et al*, 2009; Jin *et al*, 2009; Kumar *et al*, 2009; Kumar and Mayer, 2010). The 'strong' (mostly hydrophobic) lower–lower lobe contacts at AMPA and kainate receptor NTDs render ligand-induced conformation changes unlikely, although some flexibility may be present at certain AMPA receptor NTDs (Sukumaran *et al*, 2011). Compared with NMDARs where the NTDs have a leading role in allosteric modulation, in AMPA and kainate receptors, positive allosteric modulation occurs through modifications of the ABD arrangement. Compounds like cyclothiazide or ampakines enhance AMPA receptor activity by binding the ABD dimer interface and stabilizing its active conformation (Sun *et al*, 2002; Jin *et al*, 2005). Similarly, at kainate receptors, the endogenous Na^+ and Cl^- ions bind a cavity at the ABD dimer interface and favour receptor activity by preventing entry into a desensitized state (Plested *et al*, 2008).

In conclusion, our work determines for the first time a pharmacological site for positive allosteric modulation in NMDARs. In contrast to all other NMDAR ligand binding sites described so far, this site is not embedded within a single subunit but resides at a labile subunit–subunit interface, highlighting the importance of quaternary conformational changes in the control of receptor activity. The physiological and pathological relevance of the GluN2B-specific polyamine potentiation of NMDARs remains to be elucidated. *In vivo*, the polyamine site has been proposed to be partially occupied by magnesium ions, which at physiological (millimolar) concentrations potentiate NMDAR activity in a similar manner to polyamines (Paoletti *et al*, 1995; Kew and Kemp, 1998). Preclinical data indicate that polyamine administration can increase the occupancy of the polyamine modulatory site, enhance GluN2B receptor activity and improve memory in a number of cognitive tasks (Velloso *et al*, 2009; Gomes *et al*, 2010). The strong interplay between polyamine and pH sensitivities of NMDARs (with spermine potentiation being magnified by extracellular acidity) provides additional interesting hints. While extracellular pH changes during normal synaptic transmission are unlikely to be of sufficient amplitude to affect spermine potentiation significantly, the situation likely differs during pathological conditions such as stroke or ischaemia. In these conditions, pH levels of the interstitial space can fall by several tenths of a pH unit, to values as low as 6.2 (Chesler and Kaila, 1992). These changes are large enough to influence spermine potentiation of NMDARs strongly (see Traynelis *et al*, 1995 and Figure 1A). Thus, during neuronal hyper-excitability, the concomitant release of polyamines with the fall of pH_{ext} to values below 7.0 is expected to magnify greatly the extent of polyamine potentiation of NMDARs. This could exacerbate neuronal

Materials and methods

Molecular biology

The pcDNA3-based expression plasmids for rat GluN1-1a (named GluN1 herein), rat GluN2A, mouse ε2 (named GluN2B herein), rat GluN2C and rat GluN2D subunits and the sequencing procedure have already been described previously (Paoletti *et al*, 1997; Rachline *et al*, 2005). Chimeras exchanging full NTDs, GluN2A-2B(NTD), GluN2A-2B(NTD + L), GluN2B-2A(NTD) and GluN2B-2A(NTD + L), were obtained as described in Gielen *et al* (2009). Single mutants were obtained by Quikchange mutagenesis (Stratagene, La Jolla, CA). Chimeras exchanging either the NTD-ABD linkers (L) or the β6–β8 regions of GluN2A and GluN2B NTDs, as well as the subunits GluN1-4R, GluN1-4A-4R, GluN2B-4R-D206K and GluN2B-D181A-4R-D206K, were obtained by a modified protocol of the Quikchange mutagenesis strategy allowing for the insertion, deletion and replacement of large DNA fragments (up to 100 bp; Geiser *et al*, 2001). In GluN1-4R and GluN1-4A-4R, '4R' represents the residues E181, E185, E186 and E188 that were mutated in arginine and '4A' the residues D169, D170, E172 and E192 that were mutated in alanine. In GluN2B-4R-D206K and GluN2B-D181A-4R-D206K, '4R' represents the residues E191, E198, E200 and E201 that were mutated in arginine.

The plasmids for the GluN1-ΔNTD and GluN2B* subunits were a gift from Professor Jian-Hong Luo (Department of Neurobiology, Zhejiang University, China). The GluN2B* subunit represents a wild-type GluN2B subunit carrying a yellow fluorescent protein inserted at the N-terminus, upstream of the NTD, as described in Qiu *et al* (2009). The GluN1-ΔNTD subunit was coexpressed with the GluN2B* subunit because coexpression of GluN1-ΔNTD with our wild-type GluN2B subunit failed to yield functional receptors. We verified that the GluN1wt/GluN2B* receptors were still sensitive to spermine (potentiation by 200 μM spermine of 8.6 ± 0.7, $n = 4$, pH 6.5).

Electrophysiological experiments

Recombinant NMDARs were expressed in *Xenopus laevis* oocytes after coinjection of 30 nl of a mixture of cDNAs (at 10–30 ng/μl; nuclear injection) coding for various GluN1-1a and GluN2 subunits (ratio 1:1). Oocytes were prepared, injected, voltage clamped and superfused as described previously (Paoletti *et al*, 1997). Data were collected and analysed using pClamp 9.2 (Molecular Devices, Sunnyvale, CA). They were fitted using Sigmaplot 8.0 (SSPS, Chicago, IL). Error bars represent the s.d. of the mean value.

The standard external solution used for recordings at pH 7.3 contained (in mM): 100 NaCl, 0.3 BaCl₂, 5 HEPES and 2.5 KOH. The pH was adjusted to 7.3 with HCl. For recordings performed at a pH ⩽ 6.5, the concentration of HEPES was increased to compensate for the loss of buffering capacity of HEPES at acidic pH. The standard external solution contained (in mM): 60 NaCl, 0.3 BaCl₂, 40 HEPES, 2.5 KOH. The pH was first adjusted to 10.3 with NaOH to set the concentration of Na⁺ ions to ∼100 mM. Then, pH was decreased to 6.5 with concentrated HCl. In all, 10 μM DTPA was added to all the solutions to chelate contaminating zinc (Paoletti *et al*, 1997). For pH dose–response curves, solutions were prepared and analysis was performed according to Gielen *et al* (2008).

NMDAR-mediated currents were induced by simultaneous application of saturating concentrations of L-glutamate and glycine (100 μM each). Unless notified, recordings were performed at a holding potential of −60 mV. All experiments were performed at room temperature.

Recordings with spermine. Spermine powder was purchased from Sigma-Aldrich (St Louis, MO). Solutions of 200 μM spermine were made by directly diluting the powder into the standard agonist solution. When spermine sensitivity was measured at pH 8.3, spermine concentration was adjusted to 250 μM to compensate for the loss of protonation of the spermine molecule at this pH (spermine pKa₁ ∼8.0). For spermine dose–response curves, a 10- or 5-mM stock solution was made by diluting the powder into the standard external solution. The spermine solutions of different concentrations were then obtained by dilution, and agonists

(100 μM glutamate and 100 μM glycine) were added. Spermine dose–response curves were performed at a holding potential of −30 mV (to minimize spermine pore block) and at the same level of proton inhibition (96% of inhibition), namely: pH 6.50, 6.50, 6.39, 6.27 and 6.27 for receptors composed of GluN1wt and GluN2Bwt, GluN2B-2A(L), GluN2A-2B(NTD + L), GluN2A-2B(NTD) and GluN2A-2B(175–227) subunit, respectively. As revealed by applying voltage ramps on currents carried by wt GluN1/GluN2B receptors, some pore blockade is still present at −30 mV with high spermine concentrations (⩾1 mM). We measured the ratio between the spermine potentiation observed at + 50 mV (a potential at which spermine block is absent) and that measured at −30 mV to be very close to 1.0 at 1 mM spermine (1.07 ± 0.006; almost no channel block) and 1.15 ± 0.01 at 3 mM spermine ($n = 3$ cells for each condition; pH 6.5). To account for these effects and separate the voltage-dependent block from the (voltage-independent) spermine potentiation, all the spermine dose–response curves were fitted after adjusting the data points measured at 1 and 3 mM spermine with the above correction factors. For each cell, experimental points were fitted using the following Hill equation: $I_{\text{spermine}}/I_0 = 1 + a/(1 + (\text{IC}_{50}/[\text{spermine}])n_{\text{H}})$, where I_{spermine}/I_0 is the relative current, [spermine] is the spermine concentration, IC₅₀ is the concentration of spermine producing 50% of the maximal potentiation, n_{H} is the Hill coefficient and $(a + 1)$ represents the maximal potentiation at saturating spermine concentration. IC₅₀, a and n_{H} were set as free parameters. The mentioned spermine IC₅₀s and maximal potentiations are the means of the corresponding values calculated for each individual cell.

MK-801 experiments. MK-801 was purchased from Ascent Scientific (Bristol, UK) and prepared as 100 μl aliquots (in bi-distilled water) at 50 μM and stored at −20°C. MK-801 solutions of different concentrations (25–50 nM) were prepared by dilution of the 50-μM stock solution into the agonist-containing solution. MK-801 time constants of inhibition (τ_{on}) were obtained by fitting currents with a single-exponential component within a time window corresponding to 10–90% of the maximal inhibition. Each τ_{on} was then normalized to the mean τ_{on} of wild-type GluN1/GluN2B receptors measured the same day.

Methanethiosulfonate compounds. MTS compounds (Toronto Research Chemicals, North York, Ontario, Canada) were prepared as 25 μl aliquots at a concentration of 40 mM in water for 3-(triethylammonium)propylmethanethiosulfonate bromide (MTSPtrEA), or as 10 μl aliquots at 200 mM in DMSO for the cross-linker 1,2-ethanediyl bismethanethiosulfonate (M2M). Aliquots were stored at −20°C and used within 15–30 min after thawing. For functional experiments, MTS reagents were perfused in the recording chamber at a concentration of 200 μM. Functional effects of M2M on NMDAR activity were measured at pH 6.5 to maximize M2M-induced potentiation. Experiments involving MTSPtrEA were performed at pH 7.3. MTS-induced potentiations were defined as the ratio of the NMDAR current measured after washing of the MTS by the current measured before MTS application. For the kinetics of MTSPtrEA-induced potentiation, MTSPtrEA time constants of potentiation were obtained by fitting currents with a single-exponential component within a time window corresponding to 10–90% of the maximal potentiation.

Biochemical cross-linking experiments

For each construct and each condition, four oocytes expressing functional NMDARs were incubated during 30 min, at 19°C, in 100 μl of a Barth solution (in mM: 88 NaCl, 1 KCl, 0.33 Ca(NO₃)₂, 0.41 CaCl₂, 0.82 MgSO₄, 2.4 NaHCO₃, 10 HEPES, pH adjusted to 7.6 with NaOH) supplemented with gentamycin (50 μg/μl) and containing either 1% DMSO (control) or 2 mM of the bi-functional MTS cross-linking reagent. Each batch of oocytes were then homogenized, at 4°C, by back and forth pipetting with 10 μl of a lysis buffer (20 mM Tris pH 8.0; 50 mM NaCl; 1% *N*-dodecyl-β-D-maltoside; 1 mM *N*-ethylmaleimide; complete protease inhibitor cocktail tablet *Roche Complete, Mini*), until a homogenous suspension was obtained. The samples were then submitted to a first centrifugation (16 000 *g* for 5 min at 4°C), re-homogenized by pipetting and centrifuged again. Supernatants enriched in membrane proteins were collected for subsequent western blotting experiments. Samples were separated in non-reducing conditions on 3–8% SDS–PAGE gradient gels (four oocytes per lane), dry

transferred to nitrocellulose membrane and immunoblotted with an anti-GluN1 antibody (1:1000, mouse monoclonal MAB363 clone 54.1; Millipore, Billerica, MA). Protein bands were visualized using secondary goat peroxydase-linked anti-mouse antibodies (1:10 000, Jackson ImmunoResearch, West Grove, PA), with the SuperSignal West Pico Chemiluminescent Substrate (Thermo Scientific, Waltham, MA).

Supplementary data

Supplementary data are available at *The EMBO Journal* Online (http://www.embojournal.org).

Conflict of interest

The authors declare that they have no conflict of interest.

References

Armstrong N, Jasti J, Beich-Frandsen M, Gouaux E (2006) Measurement of conformational changes accompanying desensitization in an ionotropic glutamate receptor. *Cell* **127:** 85–97

Benveniste M, Mayer ML (1993) Multiple effects of spermine on *N*-methyl-D-aspartic acid receptor responses of rat cultured hippocampal neurones. *J Physiol* **464:** 131–163

Bertrand D, Gopalakrishnan M (2007) Allosteric modulation of nicotinic acetylcholine receptors. *Biochem Pharmacol* **74:** 1155–1163

Chesler M, Kaila K (1992) Modulation of pH by neuronal activity. *Trends Neurosci* **15:** 396–402

Choi YB, Lipton SA (1999) Identification and mechanism of action of two histidine residues underlying high-affinity Zn2 + inhibition of the NMDA receptor. *Neuron* **23:** 171–180

Clayton A, Siebold C, Gilbert RJ, Sutton GC, Harlos K, McIlhinney RA, Jones EY, Aricescu AR (2009) Crystal structure of the GluR2 amino-terminal domain provides insights into the architecture and assembly of ionotropic glutamate receptors. *J Mol Biol* **392:** 1125–1132

Farina AN, Blain KY, Maruo T, Kwiatkowski W, Choe S, Nakagawa T (2011) Separation of domain contacts is required for heterotetrameric assembly of functional NMDA receptors. *J Neurosci* **31:** 3565–3579

Furukawa H, Singh SK, Mancusso R, Gouaux E (2005) Subunit arrangement and function in NMDA receptors. *Nature* **438:** 185–192

Gallagher MJ, Huang H, Grant ER, Lynch DR (1997) The NR2B-specific interactions of polyamines and protons with the *N*-methyl-D-aspartate receptor. *J Biol Chem* **272:** 24971–24979

Geiser M, Cebe R, Drewello D, Schmitz R (2001) Integration of PCR fragments at any specific site within cloning vectors without the use of restriction enzymes and DNA ligase. *Biotechniques* **31:** 88–90, 92

Gielen M, Le Goff A, Stroebel D, Johnson JW, Neyton J, Paoletti P (2008) Structural rearrangements of NR1/NR2A NMDA receptors during allosteric inhibition. *Neuron* **57:** 80–93

Gielen M, Retchless BS, Mony L, Johnson JW, Paoletti P (2009) Mechanism of differential control of NMDA receptor activity by NR2 subunits. *Nature* **459:** 703–707

Gomes GM, Mello CF, da Rosa MM, Bochi GV, Ferreira J, Barron S, Rubin MA (2010) Polyaminergic agents modulate contextual fear extinction in rats. *Neurobiol Learn Mem* **93:** 589–595

Han X, Tomitori H, Mizuno S, Higashi K, Full C, Fukiwake T, Terui Y, Leewanich P, Nishimura K, Toida T, Williams K, Kashiwagi K, Igarashi K (2008) Binding of spermine and ifenprodil to a purified, soluble regulatory domain of the *N*-methyl-D-aspartate receptor. *J Neurochem* **107:** 1566–1577

Hansen KB, Furukawa H, Traynelis SF (2010) Control of assembly and function of glutamate receptors by the amino-terminal domain. *Mol Pharmacol* **78:** 535–549

He X-L, Chow D-C, Martick MM, Garcia KC (2001) Allosteric activation of a spring-loaded natriuretic peptide receptor dimer by hormone. *Science* **293:** 1657–1662

Huggins DJ, Grant GH (2005) The function of the amino terminal domain in NMDA receptor modulation. *J Mol Graph Model* **23:** 381–388

Igarashi K, Kashiwagi K (2010) Modulation of cellular function by polyamines. *Int J Biochem Cell Biol* **42:** 39–51

Jin R, Singh SK, Gu S, Furukawa H, Sobolevsky AI, Zhou J, Jin Y, Gouaux E (2009) Crystal structure and association behaviour of the GluR2 amino-terminal domain. *EMBO J* **28:** 1812–1823

Jin RS, Clark S, Weeks AM, Dudman JT, Gouaux E, Partin KM (2005) Mechanism of positive allosteric modulators acting on AMPA receptors. *J Neurosci* **25:** 9027–9036

Karakas E, Simorowski N, Furukawa H (2009) Structure of the zinc-bound amino-terminal domain of the NMDA receptor NR2B subunit. *EMBO J* **28:** 3910–3920

Kashiwagi K, Fukuchi J, Chao J, Igarashi K, Williams K (1996) An aspartate residue in the extracellular loop of the *N*-methyl-D-aspartate receptor controls sensitivity to spermine and protons. *Mol Pharmacol* **49:** 1131–1141

Kashiwagi K, Pahk AJ, Masuko T, Igarashi K, Williams K (1997) Block and modulation of *N*-methyl-D-aspartate receptors by polyamines and protons: role of amino acid residues in the transmembrane and pore-forming regions of NR1 and NR2 subunits. *Mol Pharmacol* **52:** 701–713

Kew JN, Kemp JA (1998) An allosteric interaction between the NMDA receptor polyamine and ifenprodil sites in rat cultured cortical neurones. *J Physiol* **512** (Part 1)**:** 17–28

Kumar J, Mayer ML (2010) Crystal structures of the glutamate receptor ion channel GluK3 and GluK5 amino-terminal domains. *J Mol Biol* **404:** 680–696

Kumar J, Schuck P, Jin R, Mayer ML (2009) The N-terminal domain of GluR6-subtype glutamate receptor ion channels. *Nat Struct Mol Biol* **16:** 631–638

Kunishima N, Shimada Y, Tsuji Y, Sato T, Yamamoto M, Kumasaka T, Nakashimi S, Jingami H, Morikawa K (2000) Structural basis of glutamate recognition by a dimeric metabotropic glutamate receptor. *Nature* **407:** 971–977

Lerma J (1992) Spermine regulates *N*-methyl-D-aspartate receptor desensitization. *Neuron* **8:** 343–352

Low CM, Zheng F, Lyuboslavsky P, Traynelis SF (2000) Molecular determinants of coordinated proton and zinc inhibition of *N*-methyl-D-aspartate NR1/NR2A receptors. *Proc Natl Acad Sci USA* **97:** 11062–11067

Lynch G (2004) AMPA receptor modulators as cognitive enhancers. *Curr Opin Pharmacol* **4:** 4–11

Masuko T, Kashiwagi K, Kuno T, Nguyen ND, Pahk AJ, Fukuchi J, Igarashi K, Williams K (1999) A regulatory domain (R1-R2) in the amino terminus of the *N*-methyl-D-aspartate receptor: effects of spermine, protons, and ifenprodil, and structural similarity to bacterial leucine/isoleucine/valine binding protein. *Mol Pharmacol* **55:** 957–969

Mayer ML (2006) Glutamate receptors at atomic resolution. *Nature* **440:** 456–462

McGurk JF, Bennett MV, Zukin RS (1990) Polyamines potentiate responses of *N*-methyl-D-aspartate receptors expressed in xenopus oocytes. *Proc Natl Acad Sci USA* **87:** 9971–9974

Mony L, Kew JN, Gunthorpe MJ, Paoletti P (2009a) Allosteric modulators of NR2B-containing NMDA receptors: molecular mechanisms and therapeutic potential. *Br J Pharmacol* **157:** 1301–1317

Mony L, Krzaczkowski L, Leonetti M, Goff AL, Alarcon K, Neyton J, Bertrand H-O, Acher F, Paoletti P (2009b) Structural basis of NR2B-selective antagonist recognition by N-methyl-D-aspartate receptors. Mol Pharmacol 75: 60–74

Mott DD, Washburn MS, Zhang S, Dingledine RJ (2003) Subunit-dependent modulation of kainate receptors by extracellular protons and polyamines. J Neurosci 23: 1179–1188

Niswender CM, Conn PJ (2010) Metabotropic glutamate receptors: physiology, pharmacology, and disease. Annu Rev Pharmacol Toxicol 50: 295–322

Paoletti P, Ascher P, Neyton J (1997) High-affinity zinc inhibition of NMDA NR1-NR2A receptors. J Neurosci 17: 5711–5725

Paoletti P, Neyton J (2007) NMDA receptor subunits: function and pharmacology. Curr Opin Pharmacol 7: 39–47

Paoletti P, Neyton J, Ascher P (1995) Glycine-independent and subunit-specific potentiation of NMDA responses by extracellular Mg2 + . Neuron 15: 1109–1120

Paoletti P, Perin-Dureau F, Fayyazuddin A, Goff AL, Callebaut I, Neyton J (2000) Molecular organization of a zinc binding N-terminal modulatory domain in a NMDA receptor subunit. Neuron 28: 911–925

Paoletti P, Vergnano AM, Barbour B, Casado M (2009) Zinc at glutamatergic synapses. Neuroscience 158: 126–136

Perin-Dureau F, Rachline J, Neyton J, Paoletti P (2002) Mapping the binding site of the neuroprotectant ifenprodil on NMDA receptors. J Neurosci 22: 5955–5965

Pin JP, Prezeau L (2007) Allosteric modulators of GABA(B) receptors: mechanism of action and therapeutic perspective. Curr Neuropharmacol 5: 195–201

Plested AJ, Vijayan R, Biggin PC, Mayer ML (2008) Molecular basis of kainate receptor modulation by sodium. Neuron 58: 720–735

Qiu S, Zhang XM, Cao JY, Yang W, Yan YG, Shan L, Zheng J, Luo JH (2009) An endoplasmic reticulum retention signal located in the extracellular amino-terminal domain of the NR2A subunit of N-methyl-D-aspartate receptors. J Biol Chem 284: 20285–20298

Rachline J, Perin-Dureau F, Goff AL, Neyton J, Paoletti P (2005) The micromolar zinc-binding domain on the NMDA receptor subunit NR2B. J Neurosci 25: 308–317

Rock DM, MacDonald RL (1992) Spermine and related polyamines produce a voltage-dependent reduction of N-methyl-D-aspartate receptor single-channel conductance. Mol Pharmacol 42: 157–164

Rock DM, Macdonald RL (1995) Polyamine regulation of N-methyl-D-aspartate receptor channels. Annu Rev Pharmacol Toxicol 35: 463–482

Rosenmund C, Clements JD, Westbrook GL (1993) Nonuniform probability of glutamate release at a hippocampal synapse. Science 262: 754–757

Schorge S, Colquhoun D (2003) Studies of NMDA receptor function and stoichiometry with truncated and tandem subunits. J Neurosci 23: 1151–1158

Sobolevsky AI, Rosconi MP, Gouaux E (2009) X-ray structure, symmetry and mechanism of an AMPA-subtype glutamate receptor. Nature 462: 745–756

Stoll L, Hall J, Van Buren N, Hall A, Knight L, Morgan A, Zuger S, Van Deusen H, Gentile L (2007) Differential regulation of ionotropic glutamate receptors. Biophys J 92: 1343–1349

Sugiyama S, Vassylyev DG, Matsushima M, Kashiwagi K, Igarashi K, Morikawa K (1996) Crystal structure of PotD, the primary receptor of the polyamine transport system in Escherichia coli. J Biol Chem 271: 9519–9525

Sukumaran M, Rossmann M, Shrivastava I, Dutta A, Bahar I, Greger IH (2011) Dynamics and allosteric potential of the AMPA receptor N-terminal domain. EMBO J 30: 972–982

Sun Y, Olson R, Horning M, Armstrong N, Mayer M, Gouaux E (2002) Mechanism of glutamate receptor desensitization. Nature 417: 245–253

Traynelis SF, Burgess MF, Zheng F, Lyuboslavsky P, Powers JL (1998) Control of voltage-independent zinc inhibition of NMDA receptors by the NR1 subunit. J Neurosci 18: 6163–6175

Traynelis SF, Hartley M, Heinemann SF (1995) Control of proton sensitivity of the NMDA receptor by RNA splicing and polyamines. Science 268: 873–876

Traynelis SF, Wollmuth LP, McBain CJ, Menniti FS, Vance KM, Ogden KK, Hansen KB, Yuan H, Myers SJ, Dingledine R (2010) Glutamate receptor ion channels: structure, regulation, and function. Pharmacol Rev 62: 405–496

Tsuchiya D, Kunishima N, Kamiya N, Jingami H, Morikawa K (2002) Structural views of the ligand-binding cores of a metabotropic glutamate receptor complexed with an antagonist and both glutamate and Gd3 + . Proc Natl Acad Sci USA 99: 2660–2665

Velloso NA, Dalmolin GD, Gomes GM, Rubin MA, Canas PM, Cunha RA, Mello CF (2009) Spermine improves recognition memory deficit in a rodent model of Huntington's disease. Neurobiol Learn Mem 92: 574–580

Williams K (1997) Modulation and block of ion channels: a new biology of polyamines. Cell Signal 9: 1–13

Williams K, Kashiwagi K, Fukuchi J, Igarashi K (1995) An acidic amino acid in the N-methyl-D-aspartate receptor that is important for spermine stimulation. Mol Pharmacol 48: 1087–1098

Williams K, Zappia AM, Pritchett DB, Shen YM, Molinoff PB (1994) Sensitivity of the N-methyl-D-aspartate receptor to polyamines is controlled by NR2 subunits. Mol Pharmacol 45: 803–809

Yuan HJ, Hansen KB, Vance KM, Ogden KK, Traynelis SF (2009) Control of NMDA receptor function by the NR2 Subunit amino-terminal domain. J Neurosci 29: 12045–12058

Zhang L, Zheng X, Paupard MC, Wang AP, Santchi L, Friedman LK, Zukin RS, Bennett MV (1994) Spermine potentiation of recombinant N-methyl-D-aspartate receptors is affected by subunit composition. Proc Natl Acad Sci USA 91: 10883–10887